Circulating Fluidized Bed as a Catalytic Reactor: Experimental Study

S. Ouyang, X.-G. Li, and O. E. Potter
Dept. of Chemical Engineering, Monash University, Clayton, Victoria 3168, Australia

In recent years, the circulating fluidized bed as a reactor has experienced increasing application in industry. A circulating fluidized bed (CFB) has some unique features as a chemical reactor. The performance of the CFB reactor was investigated in a 0.25-m-dia. riser system with ozone decomposition in the reactor. Both axial and radial profiles of ozone concentration are presented, as well as overall conversions under various reaction conditions. The effects of the operating conditions on the performance of the CFB reactor were examined. The experimental results show that the performance of a circulating fluidized bed as a reactor is much nearer to that of a well-mixed system than that of a plug-flow system. The effectiveness factor of the reactor seems to decrease with increase of solids holdup in the reactor.

Introduction

Methods of handling large quantities of particulate material such as coal and other minerals become of greater importance each year. The circulating fluidized bed is one of the most promising methods and it has not been well characterized in a way that permits sound assessment of potential new mineral and chemical processes.

Until now most research has been concentrated on hydrodynamics (Li and Kwauk, 1980; Weinstein et al., 1984; Rhodes and Geldart, 1987; Hartge et al., 1988; Horio, 1991) and heat transfer (Wu et al., 1989; Glicksman, 1988). Work to date has shown that the gas-solid flow in the circulating fluidized bed (CFB) riser is nonuniform, both axially and radially. It is believed that the solids holdup and its distribution in the CFB riser play a major role both when a catalyst is employed in a chemical reactor, or coal is combusted, or an inert solid is circulated as a heat carrier.

Chemical reaction gives direct information on reactor performance in contrast to any other method. However, there are only a few published experimental results dealing with catalytic reaction and these are in small-scale circulating fluidized bed reactors (Kagawa et al., 1991; Jiang et al., 1991; Bi et al., 1992; Pagliolico et al., 1992). It is therefore difficult to evaluate the effectiveness of gas-solid contacting and the types of reactor model that may be appropriate for describing CFB reactors, particularly for the larger-scale CFB reactor. The objective of the present work is to investigate the characteristic of gas-solid contacting in a circulating fluidized bed reactor at various operating conditions. Because of the simplicity in reaction kinetics (very close to first-order reaction) and negligible heat effect of reaction due to the low concentration involved, the ozone decomposition reaction was chosen as a model reaction in the present study. Experiments were conducted in a 0.25-m-dia. $\times$ 10.5-high circulating fluidized bed reactor. The effects of gas velocity and solids circulation rate on solids holdup and its axial distribution in the CFB reactor are examined. Both axial and radial profiles of ozone concentration as well as overall conversions under various reaction conditions are presented. The effects of operating conditions (mainly gas velocity and solids circulation rate) on the performance of the CFB catalytic reactor are also evaluated. This provides much needed information to improve CFB reactor modeling.

Experimental Setup and Method

The circulating fluidized bed reactor facility used in this study is shown schematically in Figure 1. It consists of a 0.254-m-ID stainless-steel riser, 10.85 m in height, with a 0.508-m-dia. stainless-steel lined mild steel downcomer. The bottom section of the riser is equipped with a riser air injector that comprises 4 $\times$ 75-mm-dia. gas inlet injectors branching from a single 125-mm-dia. ring fed from the blowers. The riser gas is supplied from two Rootes blowers. These two blowers can supply approximately 2,800 m^3/h and a maximum delivering pressure of 215 kPa (absolute). The gas flow rate is measured by an orifice plate meter situated in the exit

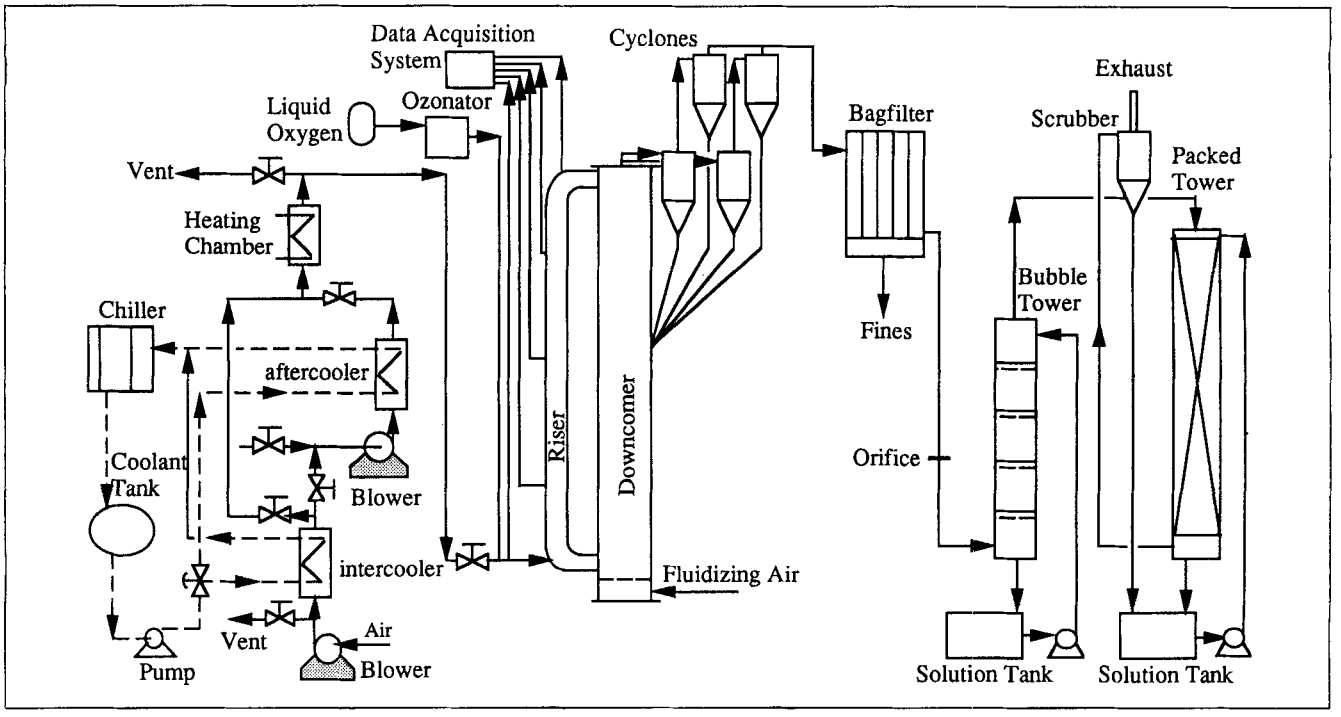

Figure 1. Circulating fluidized bed reactor system.

gas line of the unit. Because the flow rate from that measurement included the fluidizing gas of the downcomer and cyclone diplegs, it was necessary to exclude this part of the gas when determining the gas velocity of the riser. The fluidized air of the downcomer is fed into a plenum chamber at the bottom with a low-resistance distributor. To aid in the fluidizing of the downcomer, aeration points were provided at 2.5 and 5.5 m above the distributor. Pressures along the riser were measured using Honeywell micropressure sensors. The solids holdup in the riser was calculated from the pressure measurements.

The solids are fed into the riser from the downcomer through a 0.254-m knife gate valve at the bottom. The solids circulation rate is controlled by adjusting the gate valve and is measured by using the perforated flapper valve and window located in the upper section of the downcomer. The flapper valve which, when closed, allows fluidizing gas to pass upwards, will not allow solids to flow downwards. The bed level above this flapper valve rises at a rate proportional to solids circulation, and timing the rise in bed level provides a convenient means of measuring the solids circulation rates. The particles that are carried upwards through the riser are separated from the gas by the primary cyclone, which was built inside the downcomer, a pair of secondary and tertiary cyclones, and a bagfilter. The solids collected by the cyclones are returned to the downcomer. The gas is then introduced into two wash towers containing a solution of sodium thiosulfate and sodium hydroxide before discharging into the atmosphere.

Because the ozone decomposition rate constant is very sensitive to changes in gas humidity and temperature, the gas from the blowers is chilled, demisted, and heated to control the humidity and temperature. The air is preheated to the desired temperature prior to entering the riser. In order to achieve a high ozone conversion, a heating rig, used to heat the recirculated catalyst, has been installed in the bottom of the downcomer, as shown in Figure 2. The heating rig consists of nine heating elements with six of them being three-

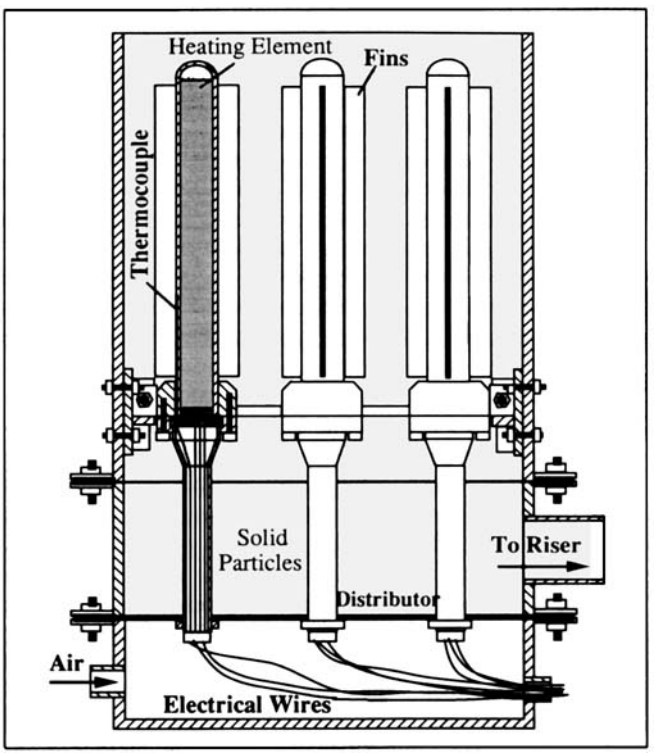

Figure 2. Layout of heating rig for solids inside the downcomer.

phase and three of them single-phase. The three-phase heating element has a 4.5-kW capacity and the single-phase heater is 3 kW. Each heating element is sheltered inside a 51-mm-ID stainless-steel tube. Eight stainless steel fins with the width of 25 mm and length of 1,000 mm were welded on the external surface of each tube. A thermocouple was grooved in the external surface of each tube. The electrical wires and thermocouple from each heater passed through a 25-mm-ID stainless-steel pipe inside the bed. The electrical wires were insulated with the ceramic beads. Each heater can be switched on separately and the single-phase heaters are connected to a proportional integral derivative (PID) controller. The solids temperature in the downcomer was monitored by three thermocouples. To reduce the heat loss through the riser and the downcomer during the operation, the entire downcomer and riser were insulated using wool insulation materials. The temperature of the solids was controlled by a 486 personal computer. The temperatures inside the riser reactor were measured by three thermocouples that are located at the bottom, the middle, and the top of the riser and recorded by a computerized data-acquisition system. The bed temperature of the reactor can be set, up to 80°C. The air used to fluidize the downcomer and cyclone diplegs was drawn from a laboratory compressed-air system. Air from the compressed-air line was introduced to the air accumulator. An automatic water drain valve was installed in the bottom of the accumulator. The air from the accumulator was introduced into the Van-Air dryer and the silica gel dryer. The dry air was then introduced into the plenum chamber of the downcomer, the diplegs of the cyclones, the lower, and upper aeration points of the downcomer. The flow rates of these streams were measured by rotameters.

Ozone is produced by an ozone generator. The ozone-rich gas from the ozonator is injected into the main gas stream through a jet pump and mixed with dry diluent air makeup stream before entering the CFB reactor. The mixing section also consists of two 90° bends. Samples taken from the probe located upstream of the riser gas injection point indicated that uniform radial ozone concentration distribution was achieved. An ultraviolet detection technique (Ouyang, 1994) was used to measure the ozone concentration. The optical part is enclosed in an aluminum case that is filled with nitrogen to exclude air and thereby prevent ozone formation. The light from an electronically modulated Philips OZ4W lamp is filtered with a type UG5 optical glass filter that passes a band of 225–400 nm. An optical beam-splitting system, which consists of one half mirror and one full mirror, is used to divide the light into two beams. The reference beam then passes through nitrogen unattenuated and the sample beam passes through a stainless-steel sample cell in which it can be attenuated by the sample gas. The cell has quartz windows on both ends and is painted matt black inside to prevent reflection. Sample gas flows continuously through the cell at a specified pressure and flow rate. The sample and reference beams are each intercepted by a Hamamatsu type R765 phototube. The phototube has a peak sensitivity at 235 nm. The combination of source and detector thus has excellent sensitivity at 253.7 nm, the wavelength of peak ozone absorption. The sample and reference beam intensities are alternately measured and the reference value continually corrects for lamp drift and so forth. This output can be monitored with a chart recorder and recorded with a computer. The ozone concentration data are collected by a computerized data-acquisition system. To obtain radial and axial ozone concentration profiles, the sampling probes are located at the heights of 0.5, 1.0, 1.5, 2.0, 3.5, 5.5, 7.0 and 10 m above the riser gas injection point and can be traversed in the radial direction. The tip of the probe is covered with a fine mesh to prevent particles entering into the sampling system. The velocity of gas sucked for sampling was less than 0.2 m/s and low enough to assume that the flow structure in the riser was not disturbed by gas sampling. The ozone meters used were regularly calibrated using the chemical method—the reaction of ozone with potassium iodide.

The catalyst used was activated equilibrium fluid cracking catalyst (FCC) with a surface mean diameter of 65 μm and a particle density of 1,380 kg/m^3. The catalyst was activated by soaking the FCC particles in a 5% solution of ferric nitrate overnight, followed by drying, then roasting at 450°C for 2 hours. However, the large quantity of catalyst needed in this project required special equipment. A rotary roaster, which was also used as a dryer, was built from stainless steel. It consists of a cylinder, rotated upon the two shafts that were driven by an electric motor. The cylinder has a diameter of 0.8 m and a length of 0.9 m. Four 45° lip flights are welded on the interior of the cylinder for lifting and showering the solids. The indirect-heat roaster, equipped with two LP gas burners, is based on batch operation. The maximum heat capacity is 250 MJ/h, capable of treating 100-kg wet FCC per batch. A thermocouple was inserted into the cylinder from the center of the front panel to monitor the solids temperature. The first-order catalytic decomposition rate constant (k_r) based on the unit volume of solid particles was measured separately in a small packed bed at a temperature and humidity similar to that in the reaction runs. Samples were taken before and after each run to check the activity.

To evaluate the possible effect of ozone reaction with the stainless-steel riser wall and sampling system, blank runs were conducted before and after each set of experiments. Because the samples taken from all probes showed a slight loss of ozone, it was believed that the loss of ozone occurs on passing through the entire sampling system, and is therefore unavoidable. To overcome this problem each probe and sample line were "calibrated" to correct the measured ozone concentration.

Results and Discussion

Hydrodynamic behavior

The cross-section average void fraction is used as a general measure to describe the overall flow pattern in the CFB riser. Hartge et al. (1986) have shown that the pressure gradient is directly proportional to the solids holdup at that height. Therefore, the measurements of time-averaged vertical pressure gradients are conveniently used to evaluate the average voidage in a section of the riser. The pressure gradient is assumed constant between two successive pressure taps. For a fully developed flow when the wall friction and local acceleration are small, the total pressure drop can be approximated to solid static head component without incurring much error:

$$\Delta P/\Delta z = \rho_s g \epsilon_s. \quad (1)$$

The pressure drops due to solids acceleration at the acceleration zone need to be considered. The acceleration loss, ΔP_{acc}, can be estimated using the following expression (Stemerding, 1962):

$$\Delta P_{acc} = U_s G_s = \frac{G_s^2}{\rho_s \epsilon_s}. \quad (2)$$

Since the injected particles would reach a final velocity at the top of the acceleration zone, the pressure drop due to acceleration is only accounted for in the initial acceleration of the solids entering the riser in the acceleration zone. The average solids holdup above this zone is calculated using Eq. 1. In the acceleration zone, the average solids holdup is estimated using the following equation:

$$\frac{\Delta P}{\Delta z} = \rho_s g \epsilon_s + \frac{G_s^2}{\rho_s \epsilon_s H_{acc}}. \quad (3)$$

The solids holdup (solids volume fraction) at some conditions, calculated from the pressure gradients measured by the micropressure sensors as a function of riser height, is shown in Figure 3. The gas velocities were relatively constant and in the range of 3.8 ~ 3.9 m/s. The total solids inventory in the CFB system was constant in all the experiments shown in this study. The solids holdup decreases with increasing height of the riser at higher solids circulation rates. Above a certain height, the solids holdup becomes relatively unchanged. The highest solids holdup occurs immediately above the gas inlet injection ports. Then the solids holdup decreases sharply with increasing bed height in the entrance region due to the particle acceleration. The acceleration zone is quite short (~ 1 m) for all cases. At the low solids circulation rate of 34 kg/m^2·s, the solids concentration is uniform along the bed height except for the entrance region. The value of the solids holdup in the lower section of the riser increases when the solids circulation rate increases. As a result the lower section of the riser becomes denser. The solids holdup in the upper section of the riser also increases with increasing the solids circulation rate, but the scale of this increment on the solids holdup is smaller than that in the lower section of the riser.

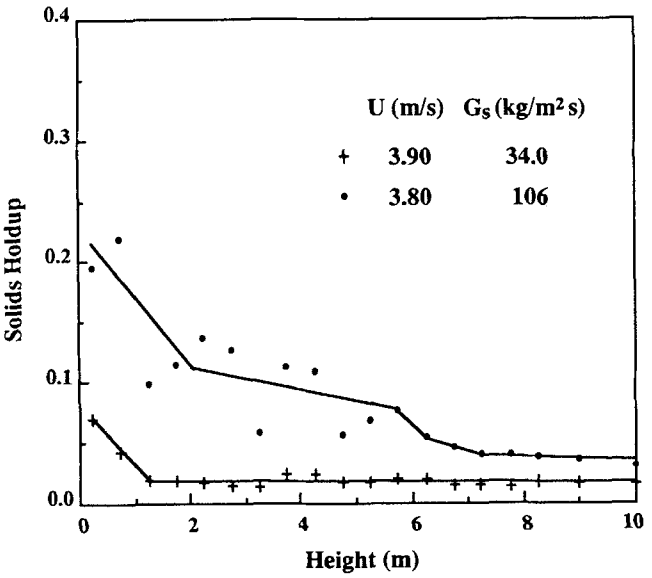

Figure 3. Axial solids holdup profiles in the riser.

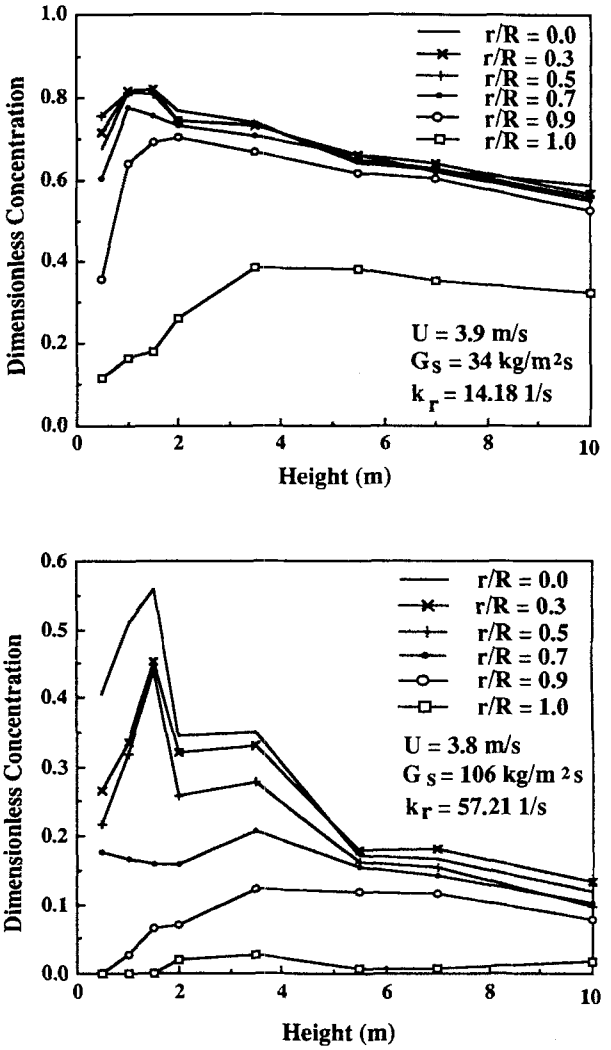

Figure 4. Axial profiles of the ozone concentration at different radial positions.

Performance of the CFB reactor

The axial ozone concentration profiles at different radial positions in the riser for different operating conditions are shown in Figure 4. Ozone concentrations in all the figures are presented in the form of "dimensionless concentration," which was defined by dividing the actual concentration by initial concentration C_0. The flatness of the axial ozone concentration profiles suggests that there exists a strong axial gas and solids mixing flow pattern in the riser reactor. The concentrations at all radial positions increase to a maximum at the height of 1.5 m before decreasing. It seems that the concentration from the gas entrance to a height up to 3 m is affected by the gas and solids mixing pattern. This is probably due to the "entrance effect" and the existing dense region in the bottom section. In the entrance region, where the bed

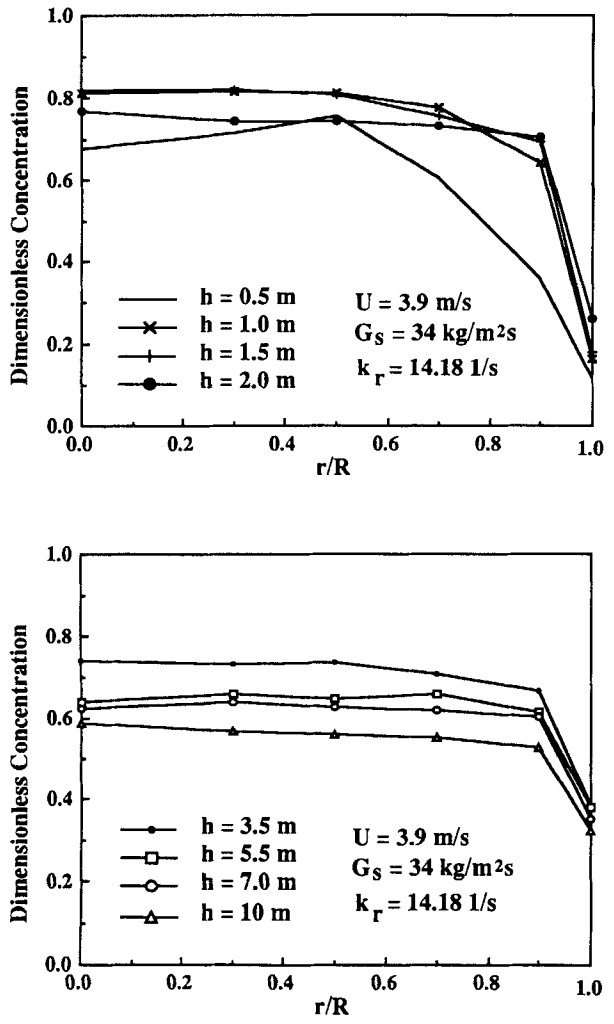

Figure 5. Radial profiles of the ozone concentration at different axial positions.

receives the internally recycled catalyst and the externally recycled catalyst stream and the feed gas stream, gas and solids mixing is extensive. The possible asymmetric flow in the entrance region and gas channeling may affect the samples taken from the bottom section of the CFB riser in the experiment. The concentration along the reactor at $r/R = 1.0$ is generally very low. This indicates that a dense layer of solids may exist near the wall. At low solids circulation rate (34 kg/m^2·s), the differences between the axial concentration profiles at $r/R = 0$ to $r/R = 0.9$ are very small. The axial profile at $r/R = 1.0$ exhibits a much lower concentration than other radial positions. At high solids circulation rate (106 kg/m^{2}s), the figure shows that the concentration decreases as the value of r/R increases. This demonstrates the direct link between the ozone concentration profile and the solids holdup and its distribution in the riser reactor as shown in Figure 3.

Radial profiles of ozone concentration at different axial positions in the CFB reactor with various operating conditions are shown in Figures 5 and 6. As can be seen from the figures, the ozone concentrations are lower near the riser wall than those close to the center of the riser, consistent with the observations of wall-flow of solids (Hartge et al., 1988; Weinstein et al., 1984). The radial concentration gradients persist over the entire height of the riser. The higher solids concentration in the wall region results in higher ozone decomposition rate as compared to that in the dilute core region. Both figures show that the ozone concentration difference between the core and the wall region at the bottom section is high. The profile in the top of the riser is flatter than that in the bottom region. The ozone concentration difference between the core and the wall region is decreased with an increase in the axial height. This corresponds to the solids holdup profiles shown in Figure 3, where the solids holdup decreases with increase in bed height.

The radial ozone concentration profiles were also measured at three angular positions for the three axial locations of 0.5, 1.0, and 1.5 m and at two angular positions for the axial locations of 2.0, 3.5, 5.5, 7.0 and 10 m in the CFB reactor. Figures 7 and 8 show the radial concentration profiles measured at different angular and axial positions at $U = 3.89$ m/s, $G_s = 75$ kg/m^2·s, and $k_r = 19.16$ s^{-1}. The results show that the ozone concentration near the wall is lower than that in the center of the reactor at all angular and axial positions. The figures also indicate strong variations in radial concen-

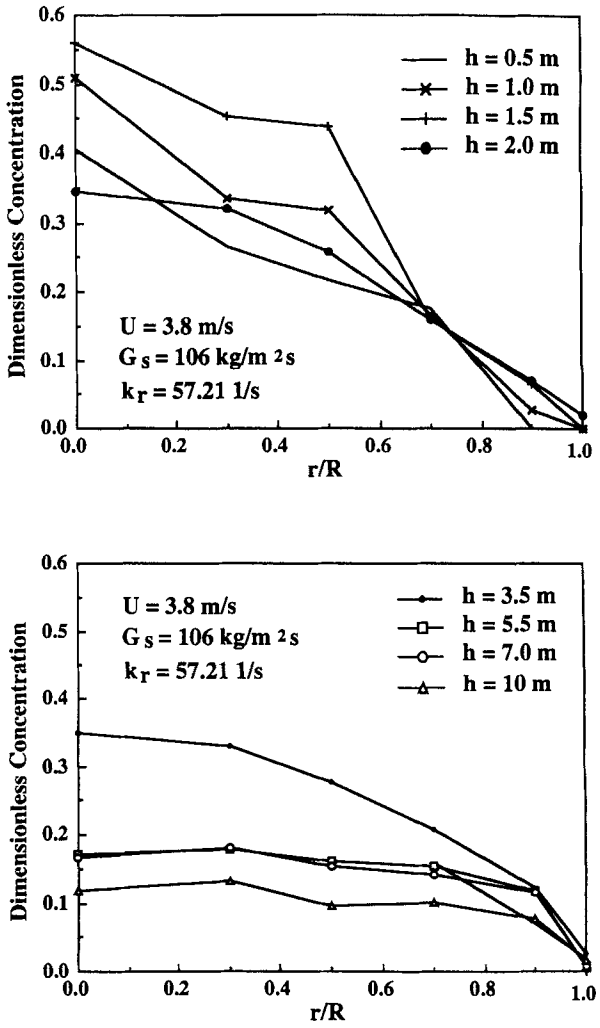

Figure 6. Radial profiles of the ozone concentration at different axial positions.

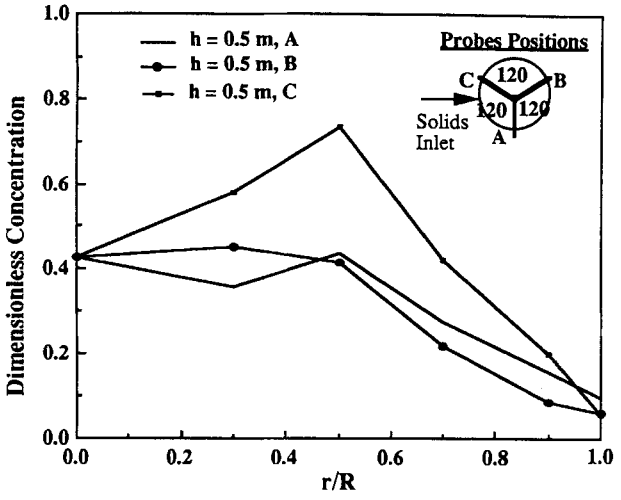

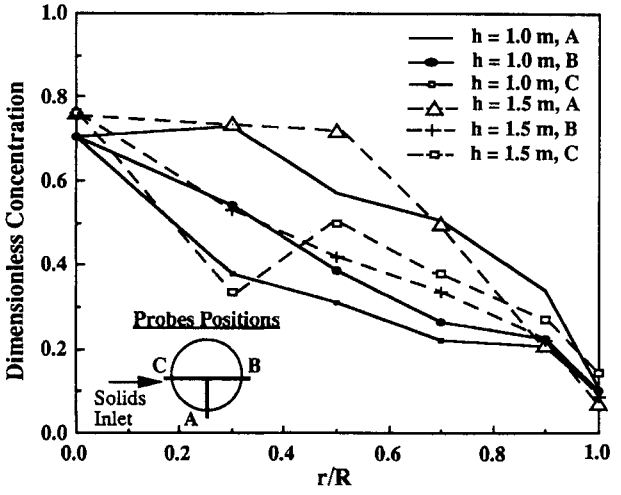

Figure 7. Radial ozone concentration profiles.

Measured at three angular positions at $U = 3.89$ m/s, $G_S = 75$ kg/m^2·s, and $k_r = 19.16$ 1/s.

tration profile with angular position, particularly at the bottom section of the CFB reactor where the gas can flow through channels. It seems that the discrepancy between different angular positions at the same axial position decreases with an increase in the height of the riser. However, more measurements would be required in order to completely characterize the concentration profile at any axial location.

The radial heterogeneity in the form of a dilute core region and a dense annular region is shown in the radial concentration profiles. The solids holdup changes from the center toward the wall. The solids holdup in the annular region is higher than that in the core region. The radial voidage distribution is much flatter in the upper section of the bed. Solids-gas flow structure exists along the CFB reactor even in the dilute conditions. The thickness of the annular region may vary in the axial direction. Possible causes for the occurrence of lateral segregation of solids and the resulting large-scale mechanical effects have been proposed by Sinclair and Jackson (1989). In most cases of interest in CFB reactors, the Reynolds number for the gas flow based on the reactor diameter is high and the flow will be turbulent at least at low solids concentrations. It is possible that the interaction between all particles and the turbulent eddies could lead to an uneven distribution of particles over the cross section (Berker and Tulig, 1986). Furthermore, in the motion of a gaseous suspension both the fluid and particle velocities have local average and random components, and various interactions depending on the two velocity fields may also have effects on the radial nonuniformity. However, the particle-phase interaction appears to be the key element required to produce lateral segregation of solids (Louge et al., 1991; Sinclair and Jackson, 1989). It was also considered that the least energy expenditure for gas flow, that is, the least resistance to gas flow through particle suspensions resulted in the aggregation of particles (Reh, 1971; Li et al., 1991).

The possible effect of the fluidizing gas in the downcomer carried into the riser by solids on the experimental results is also evaluated. There are two extreme cases: none or all of the downcomer fluidizing gas passes to the riser. If all of downcomer fluidizing gas passes to the riser, the initial ozone concentration would be diluted by over 10% at the superficial gas velocity of 2 m/s in the riser. This is an unlikely sce-

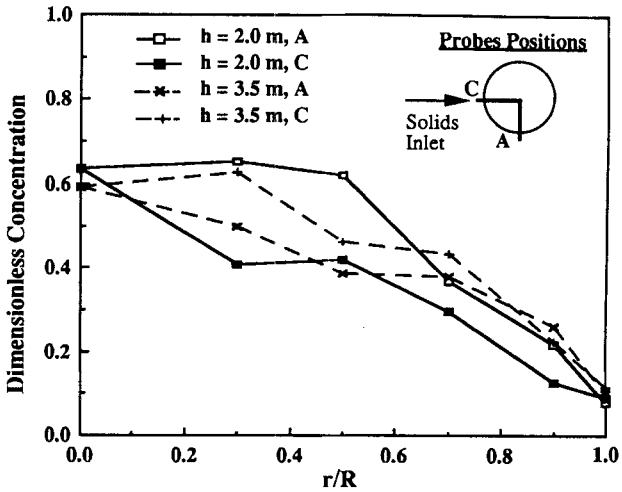

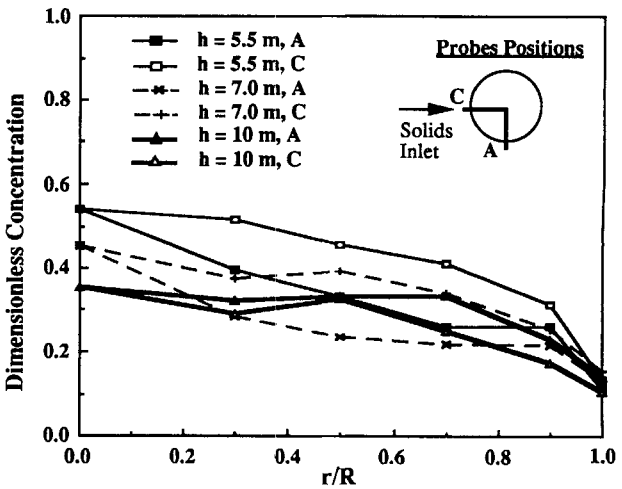

Figure 8. Radial ozone concentration profiles.

Measured at two angular positions at $U = 3.89$ m/s, $G_s = 75$ kg/m^2·s, and $k_r = 19.16$ 1/s.

Table 1. Interstitial and Pore Gas Flow at Different Conditions

Superficial gas velocity U (m/s)	2	4	6	8
Maximum solids rate $G_{s,max}$ (kg/m^2·s)	55	130	180	240
Superficial velocity of interstitial gas, U_i (m/s)	0.08	0.18	0.26	0.35
U_i/U	0.040	0.045	0.044	0.044

nario because in the experiments described here, the downcomer diameter is double that of the riser so that downwards movement of the bed is substantially slower than bubble rise velocity. In an industrial-size CFB reactor some small bubbles from the downcomer could be carried into the riser.

Since the solids entering the riser were fluidized, the gas carried by the solids may be estimated. The superficial solids velocity in the riser can be calculated by G_s/ρ_s. Hence the superficial velocity of interstitial gas carried by the solids from the downcomer to the riser would be $\epsilon G_s/[\rho_s(1-\epsilon)]$ (assuming zero slip), where ϵ is the bed porosity in the downcomer. Gas within the catalyst particle pores carried from the downcomer to the riser is estimated by assuming that the pores volume of the FCC catalyst is 50% of the total volume of the catalyst. Table 1 shows the superficial velocities of interstitial gas carried by the solids at maximum solids circulation rates under certain superficial gas velocities in this study. The bed porosity in the downcomer is assumed to be 0.6. The ratio of the superficial velocity of interstitial gas to the superficial gas velocity in the riser is in the range of 0.04 to 0.045. That means that the actual initial ozone concentration at the riser reactor was about 96% the measured concentration in the study. Therefore, the experimental values of overall conversions would be slightly lower than that in the previous calculation. The value of the Damköhler number for the corresponding conditions will also be lower. The differences between the experimental values and the conversions after the preceding correction are shown in Table 2. The comparison indicates that the difference is very small at high conversions.

The performance of the CFB reactor is related to the operating conditions (gas velocity, solids concentration, rate constant, and gas residence time). To evaluate the effects of various operating conditions on CFB reactor performance, overall ozone conversion at the top of the CFB reactor was plotted against Damköhler number $k_r'[=k_r\epsilon_s H/U]$ in Figure 9. The experimental values of the overall conversions are corrected according to the previous discussion. An ideal plug-flow reactor (PF) model and a continuous stirred tank reactor (CSTR) model are used as bases for comparison. The expressions for the overall conversion, X, are:

$$X = 1 - \exp(-k_r') \qquad \text{for plug-flow} \tag{4}$$

Table 2. Comparison of Overall Conversions With and Without Interstitial and Pore Gas

Exp. value of conv. (%)	10	20	30	40	50	60	70	80	90	95
Conv. after correction (%)	6.25	16.7	27.1	37.5	47.9	58.3	68.8	79.2	89.6	94.8

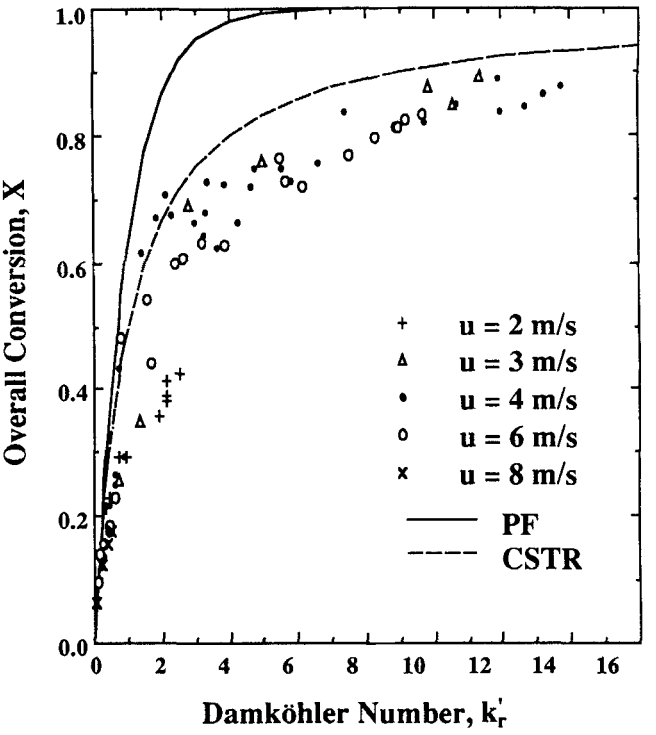

Figure 9. Effects of the Damköhler number on overall ozone conversion.

$$X = \frac{k_r'}{1+k_r'} \qquad \text{for CSTR.} \tag{5}$$

The calculated curves for the plug-flow and CSTR are also shown in Figure 9. It seems that the conversion in the CFB reactor is generally lower than that in the plug-flow reactor except at a very low Damköhler number. At a given gas velocity and reaction rate constant, the deviation from the plug-flow behavior increases with an increase of solids circulation rate (solids holdup). The extent of the deviation of the conversion can be attributed to the different gas-solid contact efficiency when the operating conditions are different. As shown previously, the gas and solids flow in the CFB reactor has a nonuniform distribution, both axially and radially. Previously published work concerning gas mixing in a CFB riser indicated that the annulus behaves like a recycling side stream as a consequence of the gas being captured and retained by the down-flowing solids (Werther et al., 1991; Amos et al., 1993). While at low solids circulation rate, the reactor mainly operates at dilute conditions, and the solids holdup remains relatively constant and low throughout the entire reactor. The dense wall region in the riser is so thin that the reaction in the wall region is insignificant. When the solids circulation rate is high, the solids holdup in the riser is high and has a nonuniform distribution. The wall region would be dense and thick, particularly at the bottom section of the reactor. The solid particles tend to form clusterlike structures at those dense regions. The existence of the clusterlike structures would reduce the gas-solid contact and ultimately affect the overall conversion of the reaction.

The effectiveness factor of the reactor, based on the pseudo-homogeneous plug-flow reactor $[=-\ln(1-X_{exp})/k_r']$,

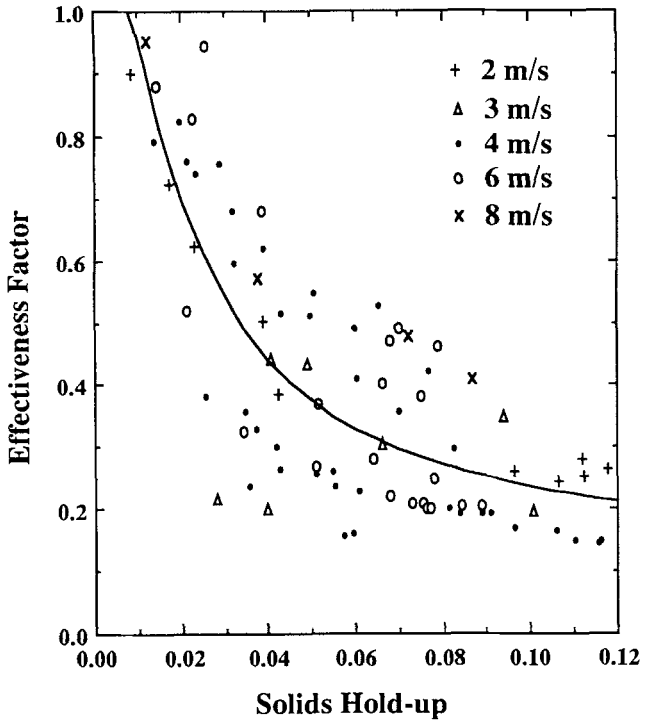

Figure 10. Effectiveness factor based on the pseudohomogeneous plug-flow model as a function of solids holdup in the reactor.

has also been plotted against the solids holdup in the reactor, as shown in Figure 10. As can be seen from the figures, the effectiveness factor approaches unity at very low solids holdup, indicating a good contact between gas and solids. But the general trend is that the effectiveness factor of the reactor decreases as the solids holdup increases. It indicates that higher solids holdup seems to be accompanied by a reduction in gas-solid contact efficiency. As an interim measure an exponential decay has been fitted, with the result also shown in Figure 10. It is not suggested, however, that this is the best way of accounting for the effect of solids holdup.

From the experimental results it was concluded that it is necessary to incorporate the effect of radial and axial nonuniformity in developing a suitable model for circulating fluidized bed reactors. Further investigation to explore the simplest core-annulus model is in progress.

Conclusions

The experimental results show that the performance of a circulating fluidized bed as a reactor is much nearer to that of a well-mixed system than that of a plug-flow system. The flatness in the axial concentration profiles measured in the reactor at various operating conditions has been shown to be caused by the combined effect of gas backmixing, radial nonuniform gas and solids flow, and the internal recirculation of solids. Radial nonuniformity in the ozone concentration distribution and in the gas and solids flow was found to exist at different axial position in the 0.254-m-ID bed with the FCC catalyst investigated in all conditions. The effectiveness factor of the reactor seems to decrease with the increase of solids holdup in the reactor. From the experimental results it was concluded that it is necessary to incorporate the effect of radial and axial nonuniformity in developing a suitable model for circulating fluidized bed reactors.

Acknowledgment

The authors gratefully acknowledge the financial support by the Australian Research Council. We also thank Mr. S. Konstantinidis and the entire technical team for their assistance with the experimental work.

Notation

C_0 = ozone concentration at the reactor entrance
D = diameter of the riser, m
g = gravitational acceleration, m/s^2
G_s = solid circulation rate, kg/m^2·s
h = distance above the riser gas entrance, m
H = height of the riser reactor, m
H_{acc} = height of acceleration zone, m
ΔP = pressure difference, Pa
r = radial coordinate, m
R = radius of the riser, m
U = superficial gas velocity, m/s
z = axial coordinate, m
ϵ_s = solids volume fraction
ρ_s = particle density, kg/m^3

Literature Cited

Amos, G., M. J. Rhodes, and H. Mineo, "Gas Mixing in Gas-Solids Risers," *Chem. Eng. Sci.*, **48**, 943 (1993).

Berker, A., and T. J. Tulig, "Hydrodynamics of Gas-Solid Flow in a Catalytic Cracker Riser: Implications for Reactor Selectivity Performance," *Chem. Eng. Sci.*, **41**, 821 (1986).

Bi, H. T., P. J. Jiang, R.-H. Jean, and L. S. Fan, "Coarse-Particle Effects in a Multisolid Circulating Fluidized Bed for Catalytic Reactions," *Chem. Eng. Sci.*, **47**, 3113 (1992).

Glicksman, L. R., "Circulating Fluidized Bed Heat Transfer," *Circulating Fluidized Bed Technology II*, P. Basu and J. F. Large, eds., Pergamon, Oxford, p. 13 (1988).

Hartge, E.-U., Y. C. Li, and J. Werther, "Analysis of the Local Structure of the Two-Phase in a Fast Fluidized Bed," *Circulating Fluidized Bed Technology*, P. Basu, ed., Pergamon, Oxford, p. 153 (1986).

Hartge, E.-U., D. Rensner, and J. Werther, "Solids Concentration and Velocity Patterns in Circulating Fluidized Beds," *Circulating Fluidized Bed Technology II*, P. Basu and J. F. Large, eds., Pergamon, Oxford, p. 165 (1988).

Horio, M., "Hydrodynamics of Circulating Fluidization—Present Status and Research Needs," in *Circulating Fluidized Bed Technology III*, P. Basu, M. Horio, and M. Hasatani, eds., Pergamon, Oxford, p. 3 (1991).

Jiang, P. J., K. Inokuchi, R.-H. Jean, H. T. Bi, and L. S. Fan, "Ozone Decomposition in a Catalytic Circulating Fluidized Bed Reactor," *Circulating Fluidized Bed Technology III*, P. Basu, M. Horio, and M. Hasatani, ed., Pergamon Press, Oxford, p. 557 (1991).

Kagawa, H., H. Mineo, R. Yamazaki, and K. Yoshida, "A Gas-Solid Contacting Model for Fast Fluidized Bed," in *Circulating Fluidized Bed Technology III*, P. Basu, M. Horio, and M. Hasatani, eds., Pergamon, Oxford, p. 551 (1991).

Li, Y., and M. Kwauk, "The Dynamics of Fast Fluidization," in *Fluidization*, J. R. Grace and J. M. Matsen, eds., Plenum, New York, p. 537 (1980).

Li, J. H., L. Reh, and M. Kwauk, "Application of the Principle of Energy Minimization to the Fluid Dynamics of Circulating Fluidized Beds," *Circulating Fluidized Bed Technology III*, P. Basu, M. Horio, and M. Hasatani, eds., Pergamon, Oxford, p. 105 (1991).

Louge, M. Y., E. Mastorakos, and J. T. Jenkins, "The Role of Particle Collisions in Pneumatic Transport," *J. Fluid Mech.*, **231**, 345 (1991).

Ouyang, S., "Circulating Fluidized Bed as a Catalytic Reactor," PhD Thesis, Monash Univ., Clayton, Victoria, Australia (1994).
Pagliolico, S., M. Tiprigan, G. Rovero, and A. Gianetto, "Pseudo-Homogeneous Approach to CFB Reactor Design," *Chem. Eng. Sci.*, **47**, 2269 (1992).
Reh, L., "Fluidized Bed Processing," *Chem. Eng. Prog.*, **67**, 58 (1971).
Rhodes, M. J., and D. Geldart, "A Model for the Circulating Fluidized Bed," *Power Technol.*, **53**, 155 (1987).
Sinclair, J. L., and R. Jackson, "Gas-Particle Flow in a Vertical Pipe with Particle-Particle Interactions," *AIChE J.*, **35**, 1473 (1989).
Stemerding, S., "The Pneumatic Transport of Cracking Catalyst in Vertical Risers," *Chem. Eng. Sci.*, **17**, 599 (1962).
Weinstein, H., M. Meller, M. J. Shao, and R. J. Parisi, "Radial Solid Density Variation in a Fast Fluidized Bed," *AIChE Symp. Ser.*, Vol. 80, No. 241, p. 117 (1984).
Werther, J., E. U. Hartge, M. Kruse, and W. Nowak, "Radial Mixing of Gas in the Core Zone of a Pilot Scale CFB," in *Circulating Fluidized Bed Technology III*, P. Basu, M. Horio, and M. Hasatani, eds., Pergamon, Oxford, p. 593 (1991).
Wu, R. L., J. R. Grace, C. J. Lim, and C. M. H. Brereton, "Suspension to Surface Heat Transfer in a Circulating-Fluidized-Bed Combustor," *AIChE J.*, **35**, 1685 (1989).

Manuscript received May 16, 1994, and revision received Sept. 9, 1994.